

# Two-qubit gates in a trapped-ion quantum computer by engineering motional modes

Ming Li,<sup>1</sup> Jason Amini,<sup>1</sup> and Yunseong Nam<sup>1</sup>

<sup>1</sup>*IonQ, College Park, MD 20740, USA*

(Dated: April 29, 2021)

A global race towards developing a gate-based, universal quantum computer that one day promises to unlock the never before seen computational power has begun and the biggest challenge in achieving this goal arguably is the quality implementation of a two-qubit gate. In a trapped-ion quantum computer, one of the leading quantum computational platforms, a two-qubit gate is typically implemented by modulating the individual addressing beams that illuminate the two target ions, which, together with others, form a linear chain. The required modulation, expectedly so, becomes increasingly more complex, especially as the quantum computer becomes larger and runs faster, complicating the control hardware design. Here, we develop a simple method to essentially remove the pulse-modulation complexity at the cost of engineering the normal modes of the ion chain. We demonstrate that the required mode engineering is possible for a three ion chain, even with a trapped-ion quantum computational system built and optimized for a completely different mode of operations. This indicates that a system, if manufactured to target specifically for the mode-engineering based two-qubit gates, would readily be able to implement the gates without significant additional effort.

## I. INTRODUCTION

Quantum computational hardware is advancing fast, with much interest and investment from across the globe [1]. Two platforms, namely, superconducting and trapped-ion quantum computers (TIQC), are in the leads today, available for a commercial use [2–5]. Unfortunately, these quantum computers are limited in their computational power, mainly due to their yet-to-mature underlying technologies that are used to implement quantum gates. A two-qubit gate, being more sophisticated over a single-qubit gate in its level of controls required, has traditionally been and is expected to continue to be the bottleneck in bettering the quality and increasing the power of quantum computational systems.

A typical TIQC, with all the control hardware required, is of substantial size comparable to an adult elephant. When building a TIQC that operates on a laser-based gate, a significant portion of the backroom consists of complicated control equipment, such as optics and electronics, for modulating optical pulses, akin to the early days of classical computers where the control hardware occupied a large physical volume of space. If we are to learn from the history of classical computer development, to accelerate the TIQC hardware development, there is likely a need to explore different technology options to realize quantum gate operations on a TIQC by shifting the technical complication in certain less mature domains of the control technology onto a more accessible, potentially new technology. By solving the backroom-size problem and streamlining the engineering effort, an eventual miniaturization of quantum computers may also be enabled.

In this paper, we take a first step towards addressing this problem by trading the complexity in modulating the optical pulses for the complexity in implementing static trapping potentials. Specifically, we explore a possibility to greatly simplify pulse modulation for a TIQC at

the expense of more complex trap voltage control and potentially more sophisticated trap design and fabrication. By demonstrating that our trade-off can readily be implemented on today’s system designed and built for a completely different mode of operations on a three-ion chain, we make a concrete progress towards a successful solution to the problem, instilling confidence that a co-design based approach between the proof-of-principle theory work we show here and the prospective hardware development could potentially advance the TIQC technology in the desirable direction.

## II. TRADITIONAL TWO-QUBIT GATES ON A TRAPPED-ION QUANTUM COMPUTER

In this section, we briefly review a two-qubit XX gate, typically used in a trapped-ion quantum computer. Specifically, we assume a hardware configuration of a linear chain of ions, each of which can be addressed with individually addressing beam(s).

An XX gate induces quantum entanglement between two trapped-ion qubits  $i$  and  $j$ , defined by the unitary operator

$$\text{XX}(\theta_{ij}) = e^{-i\theta_{ij}(\sigma_x^i \otimes \sigma_x^j)/2}, \quad (1)$$

where  $\theta_{ij}$  denotes the degree of entanglement and  $\sigma_x^{i,j}$  are the Pauli- $x$  matrices acting on the qubit space  $i$  or  $j$ . To implement such a gate, the standard de-facto approach is to use the widely adopted Mølmer-Sørensen (MS) [6, 7] protocol, which exploits the coupling between the individual qubit space and the shared motional space. Ideally, the coupling is invoked during the gate operation only, and the two spaces are decoupled from each other at the end of the gate. More concretely, this means that,

for an error budget of  $\epsilon$ , we require [8]

$$\alpha := \frac{4}{5} \sum_{p=1}^N \coth \frac{\hbar \omega_p}{2k_B T_p} (\eta_p^i{}^2 + \eta_p^j{}^2) \left| \int_0^\tau g(t) e^{i(\omega_p t + \phi_p)} dt \right|^2 < \epsilon, \quad (2)$$

where, for a linear chain with  $N$  modes coupled with the beams,  $\alpha$  denotes the residual coupling between motional modes  $p$  and ions  $i$  and  $j$  after the gate operation,  $g(t)$  is the shape of the pulse that illuminates individual ions,  $\eta_p^{i,j}$  are the Lamb-Dicke parameters,  $\tau$  is the total gate time,  $\omega_p$  is the angular mode frequency,  $\phi_p$  is the initial phase associated with mode  $p$  at time  $t = 0$ ,  $T_p$  is the temperature of the  $p$ -th mode,  $\hbar$  is the reduced Planck constant, and  $k_B$  is the Boltzmann constant. Satisfying (2) ensures the contribution to the infidelity of the gate operation from the residual mode coupling is smaller than  $\epsilon$ .

As mentioned earlier, an XX gate defined in (1) has a parameter called the degree of entanglement  $\theta_{ij}$ . A formula for  $\theta_{ij}$  is given by the sum of time-ordered double integrals, i.e.,

$$\chi_{ij} := \sum_{p=1}^N \eta_p^i \eta_p^j \int_0^\tau dt_2 \int_0^{t_2} dt_1 g(t_2) g(t_1) \sin[\omega_p(t_2 - t_1)] = \theta/4. \quad (3)$$

A fully entangling XX gate requires  $\theta_{ij} = \pi/2$ , or  $\chi_{ij} = \pi/8$ . An inexact implementation that induces uncertainty in  $\chi_{ij}$  incurs quantum computational error.

To meet these two constraints (2) and (3) and implement a high-fidelity two-qubit gate on a TIQC, a host of sophisticated schemes have been developed. For instance, given a mode-frequency spectrum, the pulse function  $g(t)$  is modulated according to the amplitude modulation (AM) [9], the frequency modulation (FM) [10], the phase modulation (PM) [11], and the power optimal AMFM [12] schemes. An important requirement to all these schemes is that one needs to ensure that the time-dependent electromagnetic (EM) wave seen by the ions follows the designed pulse shape faithfully. As the pulse shape to be implemented becomes increasingly complex, which is typically the case as we add more qubits for more powerful quantum computation or decrease the gate du-

ration for faster quantum computation, it becomes challenging to implement these schemes in practice. Consider pulse-modulation hardware design. Sampling rate, frequency and amplitude range, rise and fall time, and signal distortion can start to limit the accuracy of the modulation. The physical implementation of the modulation itself via, e.g., an acousto-optic modulator (AOM) may pose yet another challenge, as the input-output response function might not be ideal, thus hindering the accuracy of the EM wave seen by the ions.

### III. MOTIONAL MODE ENGINEERING FOR SIMPLE TWO-QUBIT GATE PULSE

In this section, we explore the idea of engineering the motional modes themselves to help simplify the pulse shape  $g(t)$ . Note the pulse shaping schemes discussed in the previous section assumes the motional modes as a fixed input parameter. Here we trade the pulse-shape complexity for overhead in engineering the mode spectrum. We show that, in return for a slightly more complex static DC trapping field that, combined with the RF drive, enables desirable control over the motional mode frequency spectrum, we can essentially eliminate the need for pulse shaping.

#### A. Gate requirement

Recall that, to implement a two-qubit gate, we need to satisfy (2) and (3). In our mode-engineering based approach, we require the mode frequency spectrum to obey

**Condition 1:**  $\omega_p \tau/4 = k_p \pi$  where  $k_p$  are positive integers.

We further require that the pulse  $g(t)$  obey

**Condition 2:**  $g(t + \tau/2) = -g(t)$  for  $t \in [0, \tau/2]$ .

Such a pulse can be viewed as two consecutive pulses of the same shape but with the opposite phases. Using these conditions, while allowing for an error  $|\delta k_p| \ll 1$  in mode frequency  $\omega_p = 4(k_p + \delta k_p)\pi/\tau$ , we can rewrite the integral in (2) as

$$\begin{aligned}
\int_0^\tau g(t)e^{i(\omega_p t + \phi_p)} dt &= \int_0^{\tau/2} g(t)e^{i(\omega_p t + \phi_p)} dt + \int_{\tau/2}^\tau g(t)e^{i(\omega_p t + \phi_p)} dt \\
&= \int_0^{\tau/2} g(t)e^{i(\omega_p t + \phi_p)} dt + \int_{\tau/2}^\tau g(t)e^{i[\omega_p(t-\tau/2) + \omega_p\tau/2 + \phi_p]} dt \\
&= \int_0^{\tau/2} g(t)e^{i(\omega_p t + \phi_p)} dt - \int_0^{\tau/2} g(t)e^{i(\omega_p t + \phi_p + 2\delta k_p \pi)} dt \\
&= (1 - e^{2i\delta k_p \pi}) \int_0^{\tau/2} g(t)e^{i(\omega_p t + \phi_p)} dt.
\end{aligned} \tag{4}$$

As  $\delta k_p \rightarrow 0$ , Eq. (4) vanishes, upperbounded by  $\mathcal{O}[\max(|\delta k_p|)]$ . Therefore, as long as  $\chi_{ij}$  in (3) evaluates to a non-zero value, we can always scale  $g(t)$  to satisfy the gate requirements (2) and (3), assuming  $\delta k_p \rightarrow 0$ . In principle, **Conditions 1** and **2** are all that we need to implement an XX gate.

### B. Pulse simplification and power optimization

To further streamline the pulse shape requirement while also lowering the power requirement, we propose the following simple procedure. We require the pulse to further satisfy

---

**Condition 3:**  $g(t) = \Omega \sin\left(\frac{2l\pi t}{\tau}\right)$  for  $t \in [0, \tau/2]$  where  $l$  is a positive integer.

This choice simplifies the generation of the optical signal, as the pulse is continuous throughout the gate duration and the initial and final signal strength at  $t = 0$  and  $\tau$  is zero. Combining now **Conditions 2** and **3**, we notice that we can separate these pulses into the groups with odd or even  $l$ . For the pulses with odd  $l$ , the signal seen by the ion at the half point of the pulse is differentiable and while the pulses with even  $l$  is not. We can derive an analytic expression for  $\chi_{ij}$  given by

$$\chi_{ij} = \begin{cases} \frac{\Omega^2 \tau^2}{2\pi} \sum_{p=1}^N \eta_p^i \eta_p^j \frac{k_p}{4k_p^2 - l^2}, & \text{if } \nexists p = 1, \dots, N \text{ that } k_p = l/2, \\ \frac{\Omega^2 \tau^2}{2\pi} \left( \eta_{p_l}^i \eta_{p_l}^j \frac{3}{8l} + \sum_{\substack{p=1 \\ p \neq p_l}}^N \eta_p^i \eta_p^j \frac{k_p}{4k_p^2 - l^2} \right), & \text{if } \exists p = 1, \dots, N \text{ that } k_p = l/2. \end{cases} \tag{5}$$

Here  $p_l$  satisfies  $2k_{p_l} = l$ . For a given set of Lamb-Dicke parameters and mode frequencies, it is straightforward to pick an  $l$  that requires the lowest  $\Omega$  to satisfy (3), which corresponds to the lowest peak-power requirement. To put it succinctly, we require

**Condition 4:**  $l$  is chosen so that the dimensionless quantity  $|\chi_{ij}/\Omega^2 \tau^2|$  is maximized according to (5).

### C. Infidelity analysis

Note there are two ways in which quantum computational errors may manifest, non-zero  $\alpha$  or inexact  $\chi_{ij}$ . Comparing to the underivable residual coupling to the mo-

---

ditional space, quantified by  $\alpha$ , which is difficult to mitigate after the gate, error in the entanglement angle quantified by  $\chi_{ij}$  is more amenable to deal with. For instance, static errors in  $\chi_{ij}$  due to imprecise mode engineering or inaccurate knowledge of  $\eta_p^{i,j}$  can readily be calibrated away by using a slightly adjusted  $\Omega$ . Inexact  $\chi_{ij}$  induced by slowly drifting, temporal noise on the mode frequencies or Lamb-Dicke parameters can be mitigated by broadband composite pulse sequences designed for a two-qubit space [13]. Thus, in the following we focus on the accuracy needed for mode engineering, *i.e.* the limit for  $|\delta k_p|$ , for a given error budget  $\varepsilon$  on  $\alpha$ .

To start, assuming non-zero  $\delta k_p$ , we write

$$\alpha = \begin{cases} \frac{l^2 \Omega^2 \tau^2}{5\pi^2} \sum_{p=1}^N \left[ \coth \left( \frac{\hbar \omega_p}{2k_B T_p} \right) \right] (\eta_p^{i^2} + \eta_p^{j^2}) \left| \frac{e^{i\phi_p} (e^{4i\delta k_p \pi} - 1)}{4(k_p + \delta k_p)^2 - l^2} \right|^2, & \text{if } l \text{ is odd,} \\ \frac{l^2 \Omega^2 \tau^2}{5\pi^2} \sum_{p=1}^N \left[ \coth \left( \frac{\hbar \omega_p}{2k_B T_p} \right) \right] (\eta_p^{i^2} + \eta_p^{j^2}) \left| \frac{e^{i\phi_p} (e^{2i\delta k_p \pi} - 1)^2}{4(k_p + \delta k_p)^2 - l^2} \right|^2, & \text{if } l \text{ is even.} \end{cases} \quad (6)$$

Assuming the motional modes are sufficiently cooled to average phonon number  $\bar{n} < 1$ , which is readily

achieved via sideband cooling schemes [14], we may let  $\coth \left( \frac{\hbar \omega_p}{2k_B T_p} \right) < 2$ . Dropping now the modulus one term  $e^{i\phi_p}$ , we can then bound  $\alpha$  in (6) by

$$\alpha < \begin{cases} \frac{2l^2 \Omega^2 \tau^2}{5\pi^2} \sum_{p=1}^N (\eta_p^{i^2} + \eta_p^{j^2}) \left| \frac{e^{4i\delta k_p \pi} - 1}{4(k_p + \delta k_p)^2 - l^2} \right|^2, & \text{if } l \text{ is odd,} \\ \frac{2l^2 \Omega^2 \tau^2}{5\pi^2} \sum_{p=1}^N (\eta_p^{i^2} + \eta_p^{j^2}) \left| \frac{(e^{2i\delta k_p \pi} - 1)^2}{4(k_p + \delta k_p)^2 - l^2} \right|^2, & \text{if } l \text{ is even.} \end{cases} \quad (7)$$

Next, if we assume  $\delta k_p$  is small, we can expand the right-

hand side to different orders of  $\delta k_p$ . This results in

$$\alpha < \begin{cases} \frac{32l^2 \Omega^2 \tau^2}{5} \sum_{p=1}^N (\eta_p^{i^2} + \eta_p^{j^2}) \frac{\delta k_p^2}{(4k_p^2 - l^2)^2} + \mathcal{O}(\delta k_p^3), & \text{if } l \text{ is odd,} \\ \alpha_0 + \frac{32l^2 \Omega^2 \tau^2 \pi^2}{5} \sum_{\substack{p=1 \\ p \neq p_l}}^N (\eta_p^{i^2} + \eta_p^{j^2}) \frac{\delta k_p^4}{(4k_p^2 - l^2)^2} + \mathcal{O}(\delta k_p^5), & \text{if } l \text{ is even,} \end{cases} \quad (8)$$

where

$$\alpha_0 = \begin{cases} 0, & \text{if } \nexists p = 1, \dots, N \text{ that } k_p = l/2, \\ \frac{2\Omega^2 \tau^2 \pi^2}{5} (\eta_{p_l}^{i^2} + \eta_{p_l}^{j^2}) \delta k_{p_l}^2 + \mathcal{O}(\delta k_{p_l}^3), & \text{if } \exists p = 1, \dots, N \text{ that } k_p = l/2. \end{cases} \quad (9)$$

We now insert  $\alpha_0$  in (9) into  $\alpha$  in (8). For a given error bound  $\varepsilon$  for  $\alpha$ , we see that the required bound on  $\delta k_p$  is much less stringent for pulses with even  $l$  than those with odd  $l$ , if there is no  $p$  such that  $k_p = l/2$ . This suggests that it may be a good idea to indeed consider this specific scenario, although in the remainder part of the manuscript we chose to continue to consider both even

and odd  $l$  pulses for completeness. Considering that calibration or error-mitigation strategies are not necessarily free, we caution that, in practice, it pays to carefully navigate the infidelity trade-off space.

An additional advantage of the proposed scheme is that the pulses we consider in our mode-engineering method can readily be adapted to suppress crosstalk

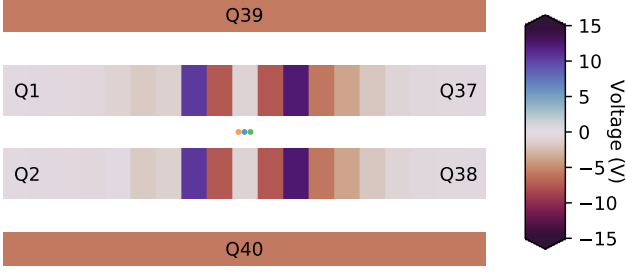


FIG. 1. Numerically solved trapping voltage color map for the “quantum” zone control electrodes of the HOA 2 trap. The three blue dots in the middle indicates where the three ion chain is trapped. The figure is not to scale.

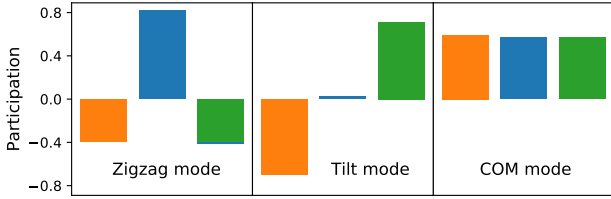


FIG. 2. Mode participation for the three-ion chain. Color orange represents ion 0, blue represents ion 1, and green represents ion 2. The zig-zag mode has the lowest mode frequency while the COM mode has the highest.

errors that arise from beam spill-over to nearby spectator ions. Note an  $XX(\theta_{ij})$  gate, implemented according to  $(U_i \otimes U_j)^{-1} XX(\theta_{ij/2})(U_i \otimes U_j) XX(\theta_{ij/2})$ , where  $U_i^{-1} \sigma_x^i U_i = -\sigma_x$ , suppresses the aforementioned crosstalk errors to a second order. Because of **Conditions 1** and **2**, the entanglement rotation angles accumulated in the first half of the gate is already the same as accumulated in the second half, i.e.,

$$\begin{aligned} & \sum_{p=1}^N n_p^i n_p^j \int_0^{\tau/2} dt_2 \int_0^{t_2} dt_1 g(t_2) g(t_1) \sin[\omega_p(t_2 - t_1)] \\ &= \sum_{p=1}^N n_p^i n_p^j \int_{\tau/2}^{\tau} dt_2 \int_{\tau/2}^{t_2} dt_1 g(t_2) g(t_1) \sin[\omega_p(t_2 - t_1)] \\ &= \chi_{ij}/2. \end{aligned} \quad (10)$$

By flipping the pulse phase on the qubit ions as in **Condition 2** and leaving the phase of the spectator ions unchanged, we can immediately implement the crosstalk suppression sequence.

#### IV. EXAMPLE: 3-ION CASE

Here we demonstrate our mode-engineering method. Specifically in this section we consider a three-ion chain,

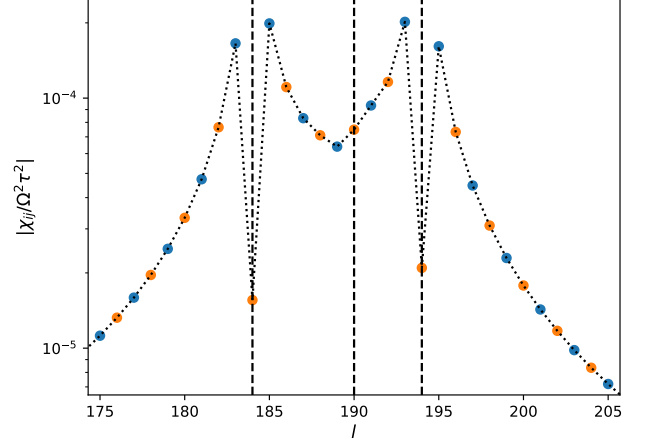


FIG. 3.  $|\chi_{ij}/\Omega^2\tau^2|$  versus  $l$  in **Condition 4** for an XX-gate implementation between ion 0 and 1. The values for even  $l$ s are shown as filled orange circles and the ones for odd  $l$ s are shown as filled blue circles. The vertical black dashed-lines correspond to the  $l = 2k_p$  of the ideal mode frequencies. We pick  $l = 193$  as the odd  $l$  pulse and  $l = 192$  as the even  $l$  pulse for their lowest power requirement respectively.

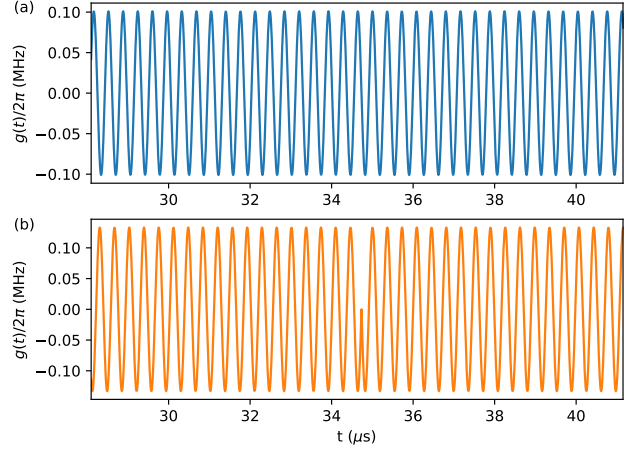


FIG. 4. Pulses of (a) odd,  $l = 193$ , and (b) even,  $l = 192$ , with the lowest power requirement respectively for an XX-gate implementation between ion 0 and 1. The pulse with odd  $l$  is infinitely differentiable at the half way point of the gate at  $t = 34.733\mu\text{s}$  while the pulse with even  $l$  has a cusp.

trapped in a Sandia High Optical Access (HOA) 2 trap [15] with individually addressing Raman beams perpendicular to the chain which couple to the three transverse modes.

To start, due to limited voltage range available in the HOA 2 trap, it is difficult to generate a scalable, analytical electrode-voltage solution that will result in a linear ion chain that satisfies **Condition 1** for arbitrarily many

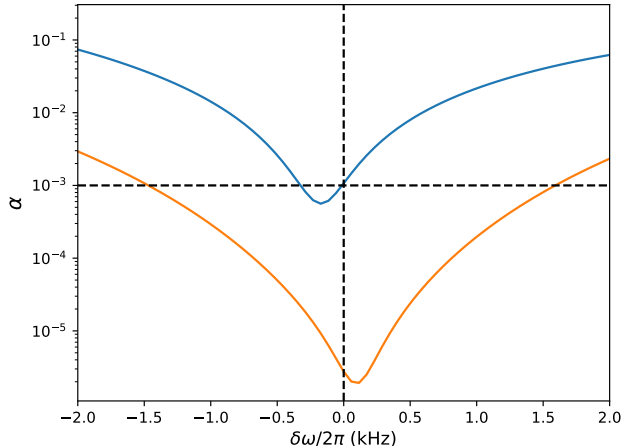


FIG. 5.  $\alpha$  as a function of common mode shift  $\delta\omega$  for the odd,  $l = 193$ , (blue) and even,  $l = 192$ , (orange) pulses with the highest powers respectively for an XX-gate implementation between ion 0 and 1.

ions. For the three-ion case, however, we can numerically optimize. Optimizing over the mode frequencies using possible DC controls provided by the HOA 2 trap to fulfill **Condition 1**, while also maintaining an ion spacing of  $\sim 4.3\mu\text{m}$  constrained by the geometry of individually addressing Raman beams, one possible solution found was the gate time of  $\tau = 69.466\mu\text{s}$  and  $k_p = 92, 95$ , and  $97$  for the zigzag, the tilt, and the center-of-mass (COM) modes, respectively.

Figure 1 shows the numerically solved trapping voltage needed on the DC control electrodes in the “quantum” zone – the zone where quantum gate operations are performed – of the HOA 2 trap. The voltage configuration traps the linear three ion chain with  $\sim 4.3\mu\text{m}$  spacing about  $71\mu\text{m}$  above the trap surface, when combined with the RF drive at  $50.6\text{ MHz}$  frequency. In order to produce the desirable mode frequencies, we apply  $289.71\text{ V}$  on the RF rails. The DC electrodes generates a slightly higher radial squeeze on the center ion than on the two end ions, which generate the zigzag mode at  $2.649 \times 2\pi\text{ MHz}$ , the tilt mode at  $2.735 \times 2\pi\text{ MHz}$ , and the COM mode at  $2.793 \times 2\pi\text{ MHz}$ . These frequencies deviates slightly from the ideal frequencies given by **Condition 1** with the  $k_p$  mentioned earlier. However, impact of the error is small, which we describe in the later part of this section. The mode participation vectors  $\nu_p^i$  are shown in Fig. 2, which are related to the Lamb-Dicke parameters by  $\eta_p^i = \nu_p^i \sqrt{\hbar/2m\omega_p}$  with  $m$  being the mass of the ions.

Without loss of generality, we now focus on implementing an XX gate between ions zero and one. We apply **Conditions 2 and 3** to  $g(t)$ , which allows us to use (5) to compute  $|\chi_{ij}/\Omega^2\tau^2|$  for different choices of  $l$ , as shown in Fig. 3. Following **Condition 4**, we pick  $l = 192$  and  $193$  for their low power requirement on  $\Omega$  for even and odd  $l$  pulses, respectively. The pulse with  $l = 192$  requires

slightly more power with  $\Omega/2\pi = 0.133\text{ MHz}$  comparing to  $0.101\text{ MHz}$  for the pulse with  $l = 193$ . The middle section of the pulses are illustrated in Fig. 4 to show the cusp for  $l = 192$  at the half-way point of the pulse, which does not exist for  $l = 193$ . However, if we opt to apply a single qubit gate rotation at that point instead of changing the optical phase in order to suppress first order cross-talk error, then the even  $l$  pulse will not have the cusp which makes it more amenable to better implement in practice.

Having determined the pulses, we next examine the stability of the fidelity of the pulses with respect to the error in mode frequency engineering and possible experimental noise. We numerically evaluate (2) using non-ideal mode frequencies, discussed earlier in the context of the limitations of the HOA 2 trap design, plus a variable common mode frequency error  $\delta\omega$  applied to all three modes. The results are shown in Fig. 5. The blue curve represents the pulse with  $l = 193$  and the orange curve represents the pulse with  $l = 192$ . At  $\delta\omega = 0$ , the infidelity due to residual motional couplings as quantified by  $\alpha$  solely comes from the static error of mode engineering or in other words the deviation of realistically generated frequencies from the ideal ones. For  $\delta\omega$  of non-zero values, the  $\alpha$ s represent infidelities due to experimental error or noises which causes the mode frequencies to from the designed ones. As expected from (8) and (9), the pulse with even  $l$  has much better infidelity compared to the pulse with odd  $l$ , owing to the  $\delta\omega^4$  dependence for even  $l$  instead of  $\delta\omega^2$  dependence for odd  $l$ . Of course, such an advantage exists when one chooses  $l \neq 2k_p$  of any mode, which is the case for our current example. The trade off is that  $\sim 30\%$  higher power requirement for  $l = 192$ , compared to that for  $l = 193$ . Considering the additional power requirement may be prohibitive in terms of implementation, the choice of  $l$  should be made on a case by case basis while fully taking the hardware limit into consideration.

## V. DISCUSSION

So far in this paper we demonstrated a method to engineer the motional modes to enable an implementation of a MS gate and showed a viability of it using an explicit example of a three-ion chain. In particular, we focused on a system manufactured for a completely different MS gate implementation architecture. This motivates us to consider if a co-design effort may be made to better implement the mode-engineering based approach in a scalable fashion. Below, we discuss this point briefly with an eye toward the technical requirements and challenges.

Note the radial and axial mode structures of a chain of ions in an ion trap can be controlled through a combination of the ion spacing and local potentials around each ion. To be more concrete, the local confining potential  $U$

of a chain of ions  $i \in [0, N)$  is

$$U(\{\mathbf{x}_i\}) = \frac{1}{2} \sum_i \mathbf{x}_i^T P_i \mathbf{x}_i + \frac{1}{2} \sum_i \mathbf{x}_i^T A_i \mathbf{x}_i + \frac{1}{2} \sum_{ij} \mathbf{x}_i^T C_{ij} \mathbf{x}_j + O(\mathbf{x}^3), \quad (11)$$

where the displacements  $\mathbf{x}_i$  are measured from the re-

spective equilibrium locations of the ions,  $A$  encodes the electrostatic potentials applied to the trapping electrodes,  $C$  encodes the Coulomb interactions between pairs of ions and depends only on the equilibrium ion locations, and  $P$  encodes the standard pseudopotential applied by the RF potentials. Up to  $O(\mathbf{x}^3)$  then, the potential can be succinctly expressed as  $U \approx \vec{\mathbf{x}}^T K \vec{\mathbf{x}}$ , where

$$K = P + A + C = \begin{bmatrix} P_0 + A_0 + C_{00} & C_{01} & \cdots & C_{0(N-1)} \\ C_{10} & P_1 + A_1 + C_{11} & \cdots & C_{1(N-1)} \\ \vdots & \vdots & \ddots & \vdots \\ C_{(N-1)0} & C_{(N-1)1} & \cdots & P_{N-1} + A_{N-1} + C_{(N-1)(N-1)} \end{bmatrix}. \quad (12)$$

Note the mode frequencies are given by the eigenvalues of  $K$ . Thus, we can control the mode structure by changing the matrix elements of  $K$ . For instance, in most ion traps,  $P$  is generated from a single source and can be scaled by changing the RF potential and/or frequency. For surface traps, and other traps with radial asymmetry, ion displacements from the RF null can further introduce changes to  $P$ . Multi-electrode traps surface traps, such as the Sandia HOA [15], provide arrays of electrodes that allow one to tune  $P$  and  $A$  and, through adjustments to the equilibrium locations,  $C$ . Optical dipole potentials can further be used to modify  $A$ . When designing a tailor-made system that operates on the basis of the mode engineered MS gate, a careful consideration then must be given to the trade-offs between ion placement, micromotion, spatial twisting of mode participation (the eigenvectors of  $K$ ), and mode spacing.

## VI. SUMMARY AND OUTLOOK

When designing traps for particular ion configurations, one can optimize the electrodes structure to match the desired potentials. With appropriate technological advancements, an increased number of trap electrodes and their shapes may be leveraged to induce the desired potentials. Further adjustments to the ion potentials could be made using potentials induced from non-trap sources as well. Whether these efforts are more amenable to higher quality quantum computer manufacturing remains to be seen. Our work provides one of the first, possible ways to redistribute the technical challenges that must be overcome to build a practical quantum computer and will certainly not be the last.

- 
- [1] E. R. MacQuarrie, C. Simon, S. Simmons, and E. Maine, The emerging commercial landscape of quantum computing, *Nat. Rev. Phys.*, **2**, 596–598 (2020).
- [2] IBM Research. Quantum Experience. <http://www.research.ibm.com/quantum/>, Accessed November 16, (2020).
- [3] Rigetti. Amazon Bracket Hardware Provider. <https://aws.amazon.com/braket/hardware-providers/rigetti/>, Accessed November 16, (2020).
- [4] <https://aws.amazon.com/braket/hardware-providers/ionq/>, Accessed November 16, (2020).
- [5] <https://www.honeywell.com/en-us/company/quantum/quantum-computer>, Accessed November 16, (2020).
- [6] K. Mølmer, A. Sørensen, Multiparticle Entanglement of Hot Trapped Ions, *Phys. Rev. Lett.* **82**, 1835–1838 (1999).
- [7] K. Mølmer, A. Sørensen, Entanglement and Quantum computation with ions in thermal motion, *Phys. Rev. A* **62**, 022311 (2000).
- [8] Y. Wu, S.-T. Wang, L.-M. Duan, Noise Analysis for High-Fidelity Quantum Entangling Gates in an Anharmonic Linear Paul Trap, *Phys. Rev. A* **97**, 062325 (2018).
- [9] S.-L. Zhu, C. Monroe, L.-M. Duan, Arbitrary-speed quantum gates within large ion crystals through minimum control of laser beams, *Europhys. Lett.* **73**, 485 (2006).
- [10] P. H. Leung, K. A. Landsman, C. Figgatt, N. M. Linke, C. Monroe, K. R. Brown, Robust 2-qubit gates in a linear ion crystal using a frequency-modulated driving force, *Phys. Rev. Lett.* **120**, 020501 (2018).
- [11] T. J. Green, M. J. Biercuk, Phase-modulated decoupling and error suppression in qubit-oscillator systems, *Phys. Rev. Lett.* **114**, 120502 (2015).
- [12] R. Blumel, N. Grzesiak, and Y. Nam, Power-optimal, stabilized entangling gate between trapped-ion qubits, <https://arxiv.org/abs/1905.09292> (2019).
- [13] Daniel C. Murphy, Kenneth R. Brown, Controlling error orientation to improve quantum algorithm success rates. *Phys. Rev. A* **99**, 032318 (2019).
- [14] J.-S. Chen, K. Wright, N. C. Pienti, D. Murphy, K. M. Beck, K. Landsman, J. M. Amini, and Y. Nam, Efficient-sideband-cooling protocol for long trapped-ion chains,

*Phys. Rev. A* **102**, 043110 (2020).

[15] P. L. W. Maunz, Sandia National Laboratories Report No. SAND2016-0796R (2016).